JACS
JOURNAL OF THE AMERICAN CHEMICAL SOCIETY

COMMUNICATION

pubs.acs.org/JACS

Size-Dependent Hydrogen Storage Properties of Mg Nanocrystals Prepared from Solution

Nick S. Norberg,[†] Timothy S. Arthur,[‡] Sarah J. Fredrick, and Amy L. Prieto*

Department of Chemistry, Colorado State University, 1872 Campus Delivery, Fort Collins, Colorado 80523, United States

Supporting Information

ABSTRACT: Mg nanocrystals of controllable sizes were prepared in gram quantities by chemical reduction of magnesocene using a reducing solution of potassium with an aromatic hydrocarbon (either biphenyl, phenanthrene, or naphthalene). The hydrogen sorption kinetics were shown to be dramatically faster for nanocrystals with smaller diameters, although the activation energies calculated for hydrogen absorption (115−122 kJ/mol) and desorption (126−160 kJ/mol) were within previously measured values for bulk Mg. This large rate enhancement cannot be explained by the decrease in particle size alone but is likely due to an increase in the defect density present in smaller nanocrystals.

A significant challenge for the widespread use of hydrogen as a practical alternative to fossil fuels is the development of safe and efficient storage materials for hydrogen.[1] Light metal hydrides, such as MgH_2, are promising candidates due to their high gravimetric and volumetric hydrogen storage densities (e.g., 7.6 wt % H_2 and 110 kg H_2/m^3 for MgH_2).[1−3] However, practical use of MgH_2 has been limited by the slow kinetics and high temperatures required for hydrogen absorption/desorption.

One successful strategy for improving the hydrogen storage properties of Mg has been to prepare nanoscale particle sizes.[4,5] This experimental approach is supported by theoretical calculations that show both Mg and MgH_2 become less stable with decreasing particle size, although MgH2 destabilizes more than Mg.[6] However, current synthetic techniques for producing nanoscale Mg, such as mechanical milling, lack the purity and size control necessary for successful hydrogen storage, or for an understanding of the relative roles of particle size versus impurities that may act as catalysts.[5,7−10] Reports of Mg nanocrystals and nanowires made by solvated metal atom dispersion followed by digestive ripening[11] or chemical vapor deposition[12] have also shown a strong improvement in the hydrogen storage properties due to decreased particle size. However size control is not possible with these synthetic approaches and they are not amenable to high throughput processing. A better understanding of the *direct* correlation between particle size and sorption kinetics can be achieved by developing a synthesis method that allows for precise control over particle size and phase purity. Herein we report the solution synthesis for the rapid preparation of pure Mg nanocrystals in gram quantities with controllable sizes. We also demonstrate that there is a clear size-dependence on the hydrogen sorption kinetics.

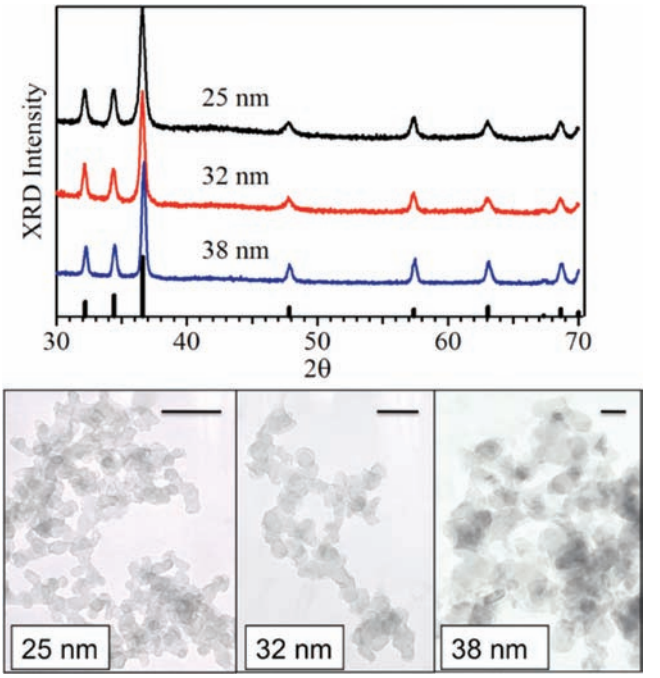

Figure 1. Powder XRD patterns (top) and TEM images (bottom) of Mg nanocrystal samples 25 nm, 32 nm, and 38 nm (scale bar = 100 nm).

Mg nanocrystals were prepared by reducing magnesocene ($MgCp_2$) dissolved in 1,2-dimethoxyethane (glyme), as an adaption of the Rieke method.[13,14] All steps were performed in a N_2 glovebox. Approximately 1.8 equiv of a reducing solution of 0.5 M potassium biphenyl (25 nm particles), potassium phenanthrene (32 nm particles), or potassium naphthalide (38 nm particles) in glyme were added to a rapidly stirring solution containing 1 equiv of $MgCp_2$ at 70 °C with a $MgCp_2$ concentration (including the reducing solutions) of 0.02 M (25 nm), 0.04 M (32 nm), or 0.08 M (38 nm), all in freshly distilled glyme. Representative amounts are shown in the Supporting Information. The reducing solutions were centrifuged prior to mixing with the $MgCp_2$ to remove undissolved particulates. After stirring and cooling of the final solution, the reaction products were centrifuged and rinsed with glyme until the supernatant solutions were clear. The final Mg product was evacuated for several hours under mild heat (50 °C) to yield a black (smallest particles) to medium gray powder (larger particles).

Received: February 26, 2011
Published: June 14, 2011

dx.doi.org/10.1021/ja201791y | *J. Am. Chem. Soc.* 2011, 133, 10679–10681

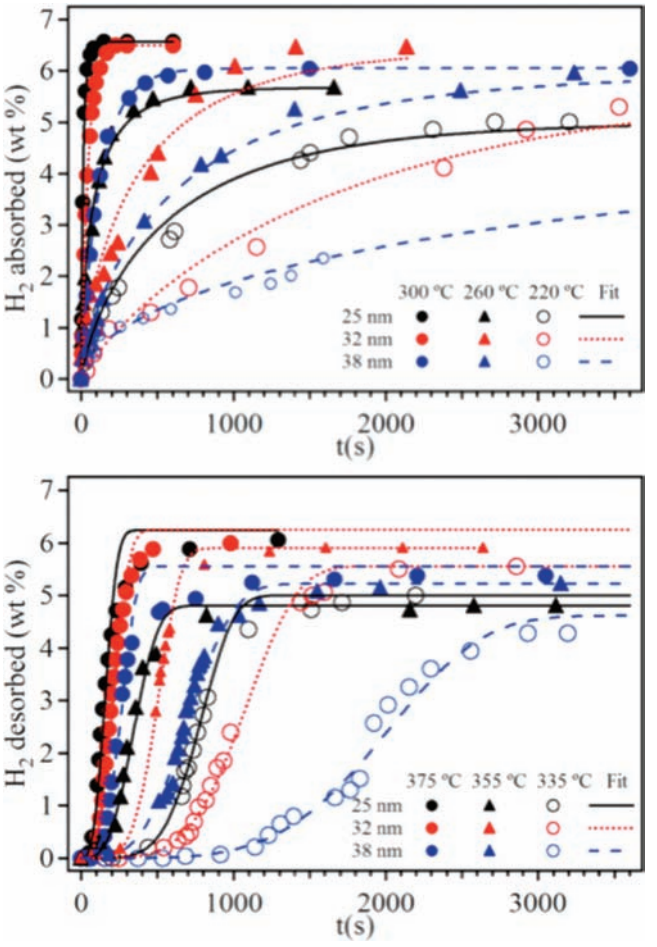

Figure 2. Hydrogen absorption (a) and desorption (b) of the Mg nanocrystal samples at different temperatures.

Figure 1 (top) shows an X-ray powder diffraction pattern of the Mg nanocrystals. All peaks match those for hexagonal Mg (JCPDS 03-065-3365) and the peak broadening increases with decreasing crystallite size, as expected. Scherrer analysis was performed on the most intense peak (36.7° 2θ) giving crystallite size estimates of 25, 32, and 38 nm. This kind of calculation should be used with caution, however, because it is not yet known if the Mg nanoparticles are single-crystalline or not, or whether significant strain is present in the as-synthesized particles. Hence, TEM imaging was used to supplement the Scherrer analysis. TEM (Figure 1, bottom) of these nanocrystals show that the particles are composed of larger aggregates that vary in shape. Analysis of >100 nanocrystals per sample yielded particle size estimates of 24 ± 7, 35 ± 10, and 72 ± 25 nm. The crystallite size estimated by Scherrer analysis is consistent with the particle size imaged in the TEM for the smaller particles. The discrepancies in estimated particle size between the XRD pattern and TEM images of the largest particles may be due to difficulties in seeing smaller particles or grains in the TEM images. Additionally the lack of contrast in the TEM images (due to Mg being such a light element) makes it challenging to distinguish individual particles from agglomerations. Zaluska et al. have shown that crystallite size is a more important factor for the kinetics of hydrogen absorption than particle size or surface area, so we used 38 nm as the size for the largest particles.[2]

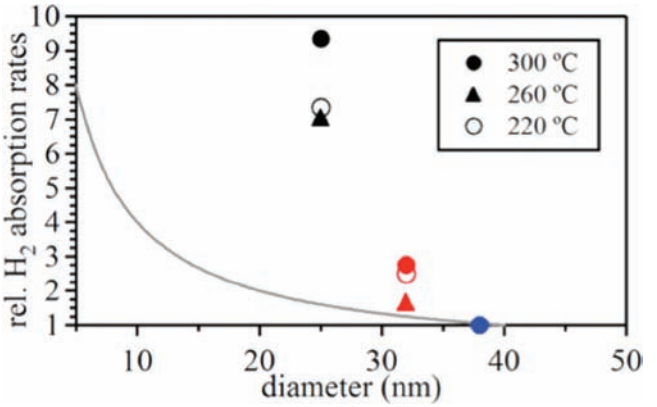

Figure 3. Hydrogen absorption rates at each temperature for Mg nanocrystal samples 1,2 and 3 relative to sample 3. The solid line follows the relationship 1/diameter.

Figure 2 shows the hydrogen absorption for Mg nanocrystals in the pressure range of 11.5 to 9.9 bar and desorption kinetics of the same particles between 0.6 to 0.2 bar, measured by pressure change using Sievert's method. The 25 nm particles absorbed 95% of the maximum capacity within 60 s at 300 °C. This is, to our knowledge, the fastest kinetics for particles of this size yet reported in the literature. The 32 and 38 nm particles absorbed 95% of their maximum capacity within 140 and 420 s, respectively. The same trend of increasing reaction time from small to large is followed at all temperatures for absorption and desorption, demonstrating the strong enhancement of kinetics by decreasing particle size. Powder X-ray diffraction (XRD) measurements of the samples after hydrogen absorption show only the β-MgH_2 phase, confirming complete conversion from Mg to MgH_2 (Figure S1). Peak broadening analysis was performed on the 25 nm particles after heating to 300 °C under vacuum for several hours, and after hydrogen absorption and desorption at 300 and 375 °C, respectively. Mg nanocrystals do not significantly change in size before absorption (27 nm) but do grow after an absorption/desorption cycle (98 nm, Figure S2). This is likely due to sample ripening at elevated temperatures.

The sorption data shown in Figure 2 were fit using the Johnson−Mehl−Avrami equation, $x_{fr} = 1 - \exp(-kt)^n$, where x_{fr} is the fraction of Mg or MgH_2 that has reacted for absorption or desorption, k is the reaction rate, t is time, and n is the reaction exponent (see Supporting Information for notes on calculations).[17,18] The fitted data are displayed (Figure 2) as lines through the data points. The desorption data were fit up to at least 60% of the desorbed fraction. Using the k values obtained from the fitted data, the activation energies (E_a) were calculated for absorption/desorption for each sample using the Arrhenius equation (Figure S3). The calculated E_a values for hydrogen absorption were 122, 118, and 115 kJ/mol H_2 for 25, 32, and 38 nm, respectively. These values are within the range of previously reported E_a values for absorption by bulk Mg (95−130 kJ/mol H_2).[15] The calculated E_a values for hydrogen desorption were 126, 131, and 160 kJ/mol H_2 for 25, 32, and 38 nm, respectively. The size of the particles does appear to slightly influence the E_a for desorption, although these energies are well within the range of previously reported values for bulk Mg (120−160 kJ/mol H_2).[15] We conclude that there is not a significant decrease in E_a for absorption or desorption with these Mg nanocrystals as compared to bulk Mg.

Despite the small differences in activation energies, there is a dramatic difference in absorption/desorption reaction rates that is much greater than what would be expected due to the size differences between the Mg nanocrystals. Figure 3 is a plot of the relative H_2 absorption rates for different size samples at each temperature, relative to the largest samples, versus diameter. The rates for 25 nm particles are over seven times higher than those for 38 nm particles.[19] This cannot be attributed to increasing surface area or decreasing diffusion distance alone, since the rate does not follow the expected inverse dependence on particle diameter, even if the TEM estimate of 72 nm is assumed for the largest particles. Defect sites have been cited as important components of Mg-based materials to improving the kinetics of H_2 sorption.[5,8] Hence, we hypothesize that there is an increase in the density of defect sites formed through the low-temperature solution synthesis described here, as the particle size decreases.

We have demonstrated that the solution synthesis of Mg nanoparticles with controlled size can provide a simple route to dramatically enhanced H_2 sorption kinetics. We anticipate that the addition of low mass percent quantities of catalyst in the future will act as grain-growth inhibitors, additionally providing a route toward reducing the activation energies for absorption/desorption in an effort to reduce the temperatures required.

■ ASSOCIATED CONTENT

Supporting Information. Additional X-ray powder diffraction patterns of Mg nanocrystals, and Arrhenius plots with notes on calculations for activation energies. This material is available free of charge via the Internet at http://pubs.acs.org.

■ AUTHOR INFORMATION

Corresponding Author
Amy.Prieto@colostate.edu

Present Addresses
[†]Lawrence Berkeley National Laboratory, Berkeley, CA.
[‡]Toyota Research Institute, Ann Arbor, MI.

■ ACKNOWLEDGMENT

We thank Colorado State University for start up funds and the CSU Microscope Imaging Network (TEM).

■ REFERENCES

(1) Schlapbach, L.; Zuttel, A. *Nature* **2001**, *414*, 353–358.
(2) Zaluska, A.; Zaluski, L.; Ström-Olsen, J. O. *Appl. Phys. A: Mater. Sci. Process.* **2001**, *72*, 157.
(3) Schuth, F.; Bogdanovic, B.; Felderhoff, M. *Chem. Commun.* **2004**, 2249.
(4) Bérubé, V.; Radtke, G.; Dresselhaus, M.; Chen, G. *Int. J. Energy Res.* **2007**, *31*, 637.
(5) Zaluska, A.; Zaluski, L.; Strom-Olsen, J. O. *J. Alloys Compd.* **1999**, *288*, 217.
(6) Wagemans, R. W. P.; Lenthe, J. H. v.; Jongh, P. E. d.; Dillen, A. J. v.; Jong, K. P. d. *J. Am. Chem. Soc.* **2005**, *127*, 16675.
(7) Huot, J.; Liang, G.; Schulz, R. *Appl. Phys. A* **2001**, *72*, 187.
(8) Sakintuna, B.; Lamari-Darkrim, F.; Hirscher, M. *Int. J. Hydrogen Energy* **2007**, *32*, 1121.
(9) Lu, J.; Choi, Y. J.; Fang, Z. Z.; Sohn, H. Y.; Rönnebro, E. *J. Am. Chem. Soc.* **2010**, *132*, 6616.
(10) Paskevicius, M; Sheppard, D. E.; Buckley, C. E. *J. Am. Chem. Soc.* **2010**, *132* (14), 5077.
(11) Kalidindi, S. B.; Jagirdar, B. R. *Inorg. Chem.* **2009**, *48*, 4524.
(12) Li, W. Y.; Li, C. S.; Ma, H.; Chen, J. *J. Am. Chem. Soc.* **2007**, *129*, 6710.
(13) Rieke, R. D.; Bales, S. E.; Hudnall, P. M.; Burns, T. P.; Poindexter, G S. *Organic Syntheses*, Coll. Vol. 6; 1988, p 845.
(14) Jeon, K.-J.; Moon, H. R.; Ruminski, A. M.; Jiang, B.; Kisielowski, C.; Bardhan, R.; Urban, J. J. *Nat. Mater.* **2011**, DOI: 10.101038.
(15) Aguey-Zinsou, K.-F.; Ares-Fernández, J.-R. *Chem. Mater.* **2008**, *20*, 376.
(16) Bogdanović, B. *Int. J. Hydrogen Energy* **1984**, *9*, 937.
(17) Fernandez, J. F.; Sanchez, C. R. *J. Alloys Compd.* **2002**, *340*, 189.
(18) Rudman, P. S. *J. Less-Common Met.* **1983**, *89*, 93.
(19) The less dramatic difference in desorption reaction rates between the different samples may be due to agglomeration effects that are likely to occur during desorption at higher temperatures.